

Poly(γ -glutamic acid) and poly(γ -glutamic acid)-based nanocomplexes enhance type II collagen production in intervertebral disc

Joana C. Antunes^{1,2,3} · Catarina Leite Pereira^{1,2,4} · Graciosa Q. Teixeira^{1,2,4} · Ricardo V. Silva^{1,2} · Joana Caldeira^{1,2,5} · Sibylle Grad⁶ · Raquel M. Gonçalves^{1,2} · Mário A. Barbosa^{1,2,4}

Received: 8 November 2015 / Accepted: 12 January 2016 / Published online: 24 November 2016
© Springer Science+Business Media New York 2016

Abstract Intervertebral disc (IVD) degeneration often leads to low back pain, which is one of the major causes of disability worldwide, affecting more than 80% of the population. Although available treatments for degenerated IVD decrease symptoms' progression, they fail to address the underlying causes and to restore native IVD properties. Poly(γ -glutamic acid) (γ -PGA) has recently been shown to support the production of chondrogenic matrix by mesenchymal stem/stromal cells. γ -PGA/chitosan (Ch) nanocomplexes (NCs) have been proposed for several biomedical applications, showing advantages compared with either polymer alone. Hence, this study explores the potential of γ -PGA and γ -PGA/Ch NCs for IVD regeneration. Nucleotomised bovine IVDs were cultured *ex vivo*

upon injection of γ -PGA (pH 7.4) and γ -PGA/Ch NCs (pH 5.0 and pH 7.4). Tissue metabolic activity and nucleus pulposus DNA content were significantly reduced when NCs were injected in acidic-buffered solution (pH 5.0). However, at pH 7.4, both γ -PGA and NCs promoted sulphated glycosaminoglycan production and significant type II collagen synthesis, as determined at the protein level. This study is a first proof of concept that γ -PGA and γ -PGA/Ch NCs promote recovery of IVD native matrix, opening new perspectives on the development of alternative therapeutic approaches for IVD degeneration.

Keywords Intervertebral disc · Organ culture · Poly(γ -glutamic acid) · Nanoparticles · Chitosan

Electronic supplementary material The online version of this article (doi:10.1007/s10856-016-5787-1) contains supplementary material, which is available to authorized users.

✉ Mário A. Barbosa
mbarbosa@ineb.up.pt

- ¹ Instituto de Investigação e Inovação em Saúde, Universidade do Porto, Rua Alfredo Allen, 208, Porto 4200-135, Portugal
- ² INEB-Instituto de Engenharia Biomédica, Universidade do Porto, Rua Alfredo Allen, 208, Porto 4200-135, Portugal
- ³ Faculdade de Engenharia, Universidade do Porto, Rua Dr. Roberto Frias s/n, Porto 4200-465, Portugal
- ⁴ ICBAS-Instituto de Ciências Biomédicas Abel Salazar, Universidade do Porto, Rua de Jorge Viterbo Ferreira 228, Porto 4050-313, Portugal
- ⁵ Instituto de Patologia e Imunologia Molecular da Universidade do Porto, Rua Alfredo Allen, 208, Porto 4200-135, Portugal
- ⁶ AO Research Institute, Davos, Clavadelstrasse 8, Davos 7270, Switzerland

1 Introduction

Low back pain (LBP) constitutes a major cause of disability to work with a global lifetime prevalence of up to 80% of the population [1–4]. It is a high socio-economic burden in western industrialized countries, implying direct costs for medical treatments and insurances [5–7]. In most cases, LBP is associated with intervertebral disc (IVD) degeneration [1, 2, 8], and may be related to genetic disorders, aging and declining cell nutrition [2, 8–10], or caused by physical trauma, abnormal weight-bearing forces and fatigue failure of the matrix [2, 9, 10].

The IVD is composed of: (i) a central part, the nucleus pulposus (NP); (ii) a peripheral region, the annulus fibrosus (AF); and (iii) cartilaginous endplates (CEPs), that superiorly and inferiorly confine the AF and NP and constitute an interface with the vertebral bodies (VBs) [3, 4, 6]. IVD degeneration is a process characterised by loss of

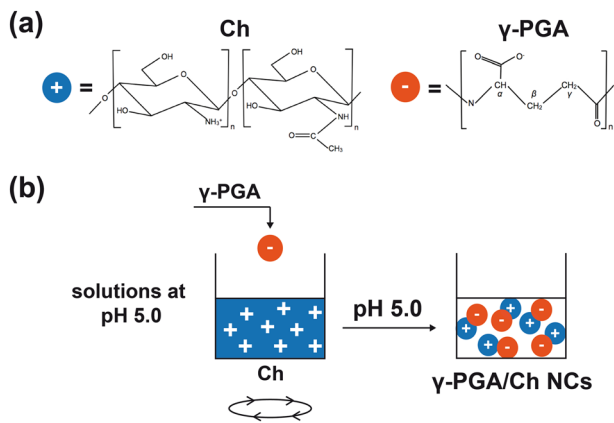


Fig. 1 **a** Molecular units of the polymers used to form the nanocomplexes (NCs): Chitosan (Ch, *left*), as a polycation, and poly(γ -glutamic acid) (γ -PGA, *right*), as a polyanion. **b** Schematics of γ -PGA/Ch NC preparation. NCs were obtained by complex coacervation driven by electrostatic interaction at pH 5.0, upon addition of a γ -PGA solution to a Ch solution under high stirring at RT. Counterions and polyions conformation were omitted for clarity (adapted from (55, 56) [59, 60]) (color figure online)

proteoglycans and increased amount and crosslinking of type I collagen accompanied by a decrease of type II collagen (Col II) in the NP. This disturbed matrix turnover is followed by a reduction of tissue hydration, which hampers its mechanical properties. As the NP becomes unable to evenly re-distribute compressive forces between the VBs, those are transferred non-uniformly to the surrounding AF, culminating in a progressive structural IVD deterioration, accompanied by vascular and neural ingrowths [2, 3, 7, 11].

Nowadays, available treatments for IVD degeneration range from conservative to surgical treatments, depending on the degeneration stage [3, 12]. However, these options fail to restore IVD structure and mechanical function [3, 7], because they do not target the underlying disease mechanisms, neither do they cease the progression of IVD degeneration.

Novel strategies able to achieve a homeostatic adjustment and tissue regeneration are being actively pursued [3, 4, 13]. Strategies based on the injection of mitogens, morphogens, anti-catabolic and/or intercellular regulators to modulate resident cell proliferation/differentiation, matrix synthesis and/or down-regulate catabolic and inflammatory processes are being investigated [14, 15]. Examples of such active biomolecules include transforming growth factor beta-1 (TGF- β 1) [16, 17] and platelet-rich plasma (PRP - a cocktail of growth factors) [18, 19]. On the other hand, small-scaled particles are starting to emerge as alternative approaches for IVD regeneration. Their size enables them to influence cellular processes (particularly at the nano-scale [20, 21]). Since they correlate with structural sizes of biological components [22] and are able to pass through biological barriers [23], being internalised into target cells [24].

Fullerol nanoparticles, in particular, were able to decrease IVD degenerative features in human cells and rabbit tissue [25]. In turn, poly(*L*-glycolic acid) microspheres coated with heparinized nanoparticles that release TGF- β 3 and dexamethasone were shown to enhance PG accumulation in rat IVDs [26].

Moreover, the discovery of new biomaterials mimicking the properties of healthy IVD has also been encouraged [27]. Poly(γ -glutamic acid) (γ -PGA) is a poly(amino acid) that recently called attention for cartilage regeneration: γ -PGA-containing scaffolds were shown to support rat chondrocyte culture [28] and γ -PGA injections were patented for the treatment of degenerative joint diseases [29]. In addition, our group recently showed that γ -PGA-supplemented medium enhanced the production of cartilaginous matrix by human mesenchymal stem/stromal cells (MSCs) [30]. Since the IVD comprises chondrocyte-like cells and skeletal progenitors [31, 32] with close resemblance to bone marrow-derived MSCs [32–36], we hypothesise that γ -PGA can recover the healthy IVD ECM in a nucleotomised ex vivo IVD model. Other attractive features of γ -PGA (such as non-immunogenicity and biodegradability) have also been previously described [30]. On the other hand, γ -PGA/chitosan (Ch) polyelectrolyte complexes (PECs) have the ability to improve intrinsic properties shown by each counterpart on its own (e.g., cytocompatibility and hydrophilicity [37–41]), enhance bulk properties (e.g., mechanical properties [42, 43]) and also act as delivery systems with improved characteristics (e.g., pH-responsiveness [44–48], higher loading efficiency [44, 49] and effectiveness [40, 49]). As nanocomplexes (NCs), different γ -PGA/Ch PECs have shown an added value in different applications [50–53]. In particular, γ -PGA/Ch NCs previously developed by our group [54, 55] were recently proposed as an effective anti-inflammatory drug delivery system that successfully reduced macrophage activation [54].

In this regard, the present study explored the potential of γ -PGA (in its soluble form) and γ -PGA/Ch NCs self-assembled through electrostatic interactions, to regenerate a nucleotomised bovine IVD using an ex vivo organ culture system. The ex vivo model used was previously described [56, 57], and has the advantages of being highly reproducible and mimicking early IVD degeneration through loss of NP, while maintaining AF integrity [57].

2 Experimental section

2.1 Materials

Ch (France-Chitine) was purified as described in Antunes et al. [58]. Ch with a degree of acetylation (DA) of

$12.8 \pm 0.4\%$ (determined by Fourier transform infrared spectroscopy with KBr pellets (FTIR-KBr)), and a molecular weight (M_w) of 538 ± 74 kDa, (determined by size-exclusion chromatography), was selected. γ -PGA has been produced by *Bacillus subtilis* and purified as described in Pereira et al. [55]. γ -PGA with low molecular weight (10–50 kDa), high purity grade (>99%), and a D-/L-glutamate ratio of 50–60/50–40% was used [58]. The endotoxin levels of Ch and γ -PGA, below the limit 0.5 EU/mL [59], were controlled by the Limulus Amebocyte Lysate (LAL) QCL-1000 kit (Cambrex/Lonza).

2.2 Preparation of γ -PGA/Ch NCs at pH 5.0

γ -PGA/Ch NCs were prepared as previously described (as illustrated in Fig. 1) [54, 55]. Briefly, γ -PGA/Ch NCs were obtained through complex coacervation, by dropping γ -PGA solution (0.2 mg/mL) into a stirring Ch solution (0.2 mg/mL), both prepared in 0.05 M Tris-HCl buffer containing 0.15 M NaCl, using a 1 mL syringe in a syringe pump (KD Scientific Inc., Holliston, U.S.A.) at constant speed (3.6 μ L/s) and room temperature (RT). Ch solution was obtained by diluting a Ch stock solution (5 mg/mL Ch in 0.2 M CH_3COOH). The solutions pH was adjusted to 5.0 using HCl or NaOH before the assembly.

2.3 Preparation of γ -PGA/Ch NCs at pH 7.4

γ -PGA/Ch NCs prepared at pH 5.0 were centrifuged (15000 rpm, RT) for 30 min, 2 h after initial preparation. γ -PGA/Ch NCs from the pellet were concentrated 10 times in the buffer solution at pH 5.0 (Supplementary Fig. S1). Concentrated γ -PGA/Ch NCs were then diluted 1 : 10 in cell culture medium (high-glucose Dulbecco's Modified Eagle Medium (DMEM; Gibco)) supplemented with 2% Fetal Bovine Serum (FBS; Gibco), 1% penicillin/streptomycin (P/S; Gibco), 1% Insulin-Transferrin-Selenium supplement (ITS; BD Becton Dickinson) and 0.1% Fungizone (Amphotericin B; PAA), a composition previously described for IVD organotypic cultures [55, 57]) at pH 7.4.

2.4 Characterisation of γ -PGA/Ch NCs by dynamic and electrophoretic light scattering (DLS and ELS) and transmission electron microscopy (TEM)

The size (d), polydispersity index (PDI), mean count rate (mcr) and surface electrical charge (ζ potential) were determined using a Zetasizer Nano ZS (Malvern Instruments, U.K.) equipped with a 4 mW HeNe laser beam with a wavelength of 633 nm and a scattering angle of 173° (for size measurements) and 13° (for ζ potential measurements). Size and ζ potential values were automatically calculated through the DTS Nano v.6.30 software, using the

Stokes-Einstein equation or the Henry equation with the Smoluchowski approximation. The dispersion solution used was the solvent in which the NCs were formed, i.e., 0.05 M Tris-HCl buffer with 0.15 M NaCl. For the mean count rate, the attenuator and measurement position were fixed at the 8 and 3 mm, respectively, which were the automatically obtained values for the γ -PGA/Ch NCs prepared as described in Fig. 1. Disposable solvent resistant micro cuvettes or folded capillary cells with gold-plated electrodes (Malvern) were used. Data were acquired at 20 °C, with three repetitions for each sample. The morphology of the NCs was observed using a transmission electron microscope (TEM) JEM 1400 (80 kV; Jeol, Japan) with an OriusTM SC1000 Digital Camera (Gatan, U.S.A.). Samples were prepared by placing 10 μ L of the NCs suspension onto a 400 μ L mesh copper grid coated with carbon (EMS). Two minute after deposition, the grid was tapped with a filter paper and negatively stained with uranyl acetate (EMS) for 10 s. TEM images were obtained with different magnifications.

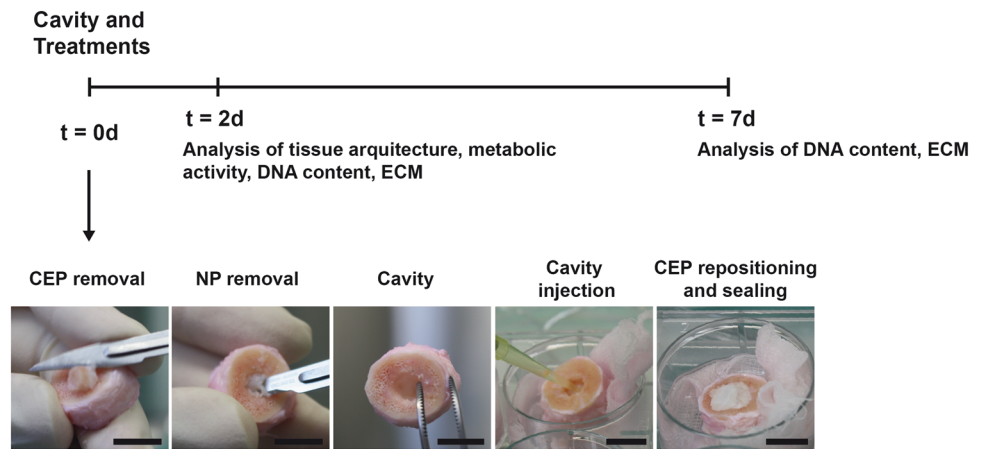
2.5 Preparation of fluorescent Ch (ftCh) and fluorescent γ -PGA/Ch NCs (γ -PGA/ftCh NCs)

Fluorescent nanoparticles were prepared according to Gonçalves et al. [54]. Briefly, Ch was labelled with fluorescein isothiocyanate (FITC) with 5% modification (5% of amine groups with FITC), whereby 100 mg of dried Ch were dissolved in 100 mL of 1% v/v CH_3COOH at 4 °C until complete dissolution. FITC (11 mg to achieve 5% modification) was dissolved in 100 mL of methanol. Both solutions (Ch and FITC) were mixed at constant stirring, protected from light, for 3 h. The FITC-labelled Ch (ftCh) was then precipitated with 0.5 M NaOH and washed with ultrapure water until no fluorescence was detected in the supernatant. ftCh was then lyophilized, dried and weighted. γ -PGA/ftCh NCs (ftNCs) were prepared as previously described.

2.6 Quantification of γ -PGA/ftCh NCs internalisation by NP cells

To evaluate the capacity of ftNCs internalisation by IVD cells, NCs were incubated with IVD cells previously isolated from bovine IVD tissue. Six bovine caudal IVDs of a young adult animal (age < 2 years old) were collected within 3 h after slaughter from a local abattoir (Carnes Landeiro S.A., Nine, Portugal), with the ethical approval of the Portuguese National Authority for Animal Health. Each NP tissue sample was dissected into 2–3 mm³ fragments and enzymatically digested for 2 h in 1.0 mg/mL collagenase type I (Sigma-Aldrich) in DMEM, at 37 °C, under agitation (50 rpm) and humidified atmosphere of 5% v/v CO₂ in air. Supernatant was passed through a 40 μ m filter (BD Falcon) to remove tissue debris. Cells were collected by

Fig. 2 Intervertebral discs (IVDs) isolated from bovine tails. After removal of a portion of cartilaginous endplate (CEP) (~4–8 mm³) and nucleus pulposus (NP) (50–100 cm³), a cavity was created and filled with different solutions. Each removed CEP was then repositioned and sealed with cement. Scale bars represent 1 cm (adapted from (57, 58) [61, 62]) (color figure online)



centrifugation at 400 g for 7 min. ftNCs (0.7 mg/mL) were added to an IVD cell suspension at a concentration of 10% v/v in cell culture medium. Three hours later cells were fixed in 1% PFA and quantified by standard flow cytometry (FACSCalibur™ system, Becton Dickinson, NJ, U.S.A.) and imaging flow cytometry (ImageStream®, AmnisMillipore, MA, U.S.A.). Cell concentration and time point for analysis were selected based on our previous work with *in vitro* studies using an anti-inflammatory treatment on activated macrophages (55) [54]. Cells incubated without nanoparticles were used as control. ftCh fluorescence was assessed in Channel 2 (505–560 nm) and at least 5000 events were collected in a FACSCalibur. FACS data was analysed using FlowJo (version 8.7). For imaging flow cytometry, samples were collected in Image Stream (Amnis) and analysis was performed in IDEAS software (Amnis). An internalisation mask was applied to determine the percentage of cells with higher fluorescence on the inside rather than on the cell membrane.

2.7 Harvest of bovine IVD tissue

IVDs with CEPs were isolated from young (<1 year old) bovine tails ($n = 6$) obtained from the same slaughterhouse. Seven caudal IVDs from each bovine tail were harvested based on a protocol previously described [56, 60]. Briefly, the caudal IVDs with CEP were removed using a circular saw (Mini grinder DM-130A-1; Dremel, U.S.A.) with parallel cuts. The CEPs were washed afterwards with phosphate-buffered saline (PBS) solution (pH = 7.4) using a 50 mL syringe connected to a 21 G needle. Under sterile conditions, IVDs were incubated sequentially in 1/10/1% of penicillin/streptomycin (P/S; Gibco) in a PBS solution (pH = 7.4) for 1/10/1 min, respectively. Then, IVDs were placed in 6-well plates, incubated with the aforementioned cell culture medium and placed overnight in a humidified atmosphere with 5% CO₂ at 37°C.

2.8 Ex vivo model of IVD organotypic culture

An *ex vivo* organotypic culture of IVD with CEP (as described in Pereira et al. [56]) was used to inject different solutions (Fig. 2). Briefly, a circular cavity of 4–8 mm³ was made in the CEP using a blade. The portion of each CEP was removed and kept in PBS with 1% P/S, while part of the NP (50–100 mm³ of tissue) was removed using another blade. The cavity created was filled (50 μL) with the following solutions:

- 1) γ -PGA/Ch NCs (0.4 mg/ml) in 0.05 M Tris-HCl with 0.15 M NaCl buffer (solvent pH 5.0);
- 2) γ -PGA/Ch NCs (0.4 mg/ml) in cell culture medium (solvent pH 7.4);
- 3) γ -PGA (0.2 mg/mL) in cell culture medium;

Additional experimental conditions included the respective controls with solvent at both pHs. The parameters evaluated were compared with those from intact IVDs obtained immediately after isolation (fresh).

Subsequently, each removed CEP was repositioned, sealed with cement (poly(methyl methacrylate) (PMMA), Vertecem™ V Cement Kit, Synthes) and incubated for 30 min at 37°C, allowing the cement to dry. Next, IVDs were placed in 6-well plates with the previously mentioned cell culture medium for 2 or 7 days in a humidified atmosphere with 5% CO₂ at 37°C. Media were changed every 2 days.

2.9 NP Haematoxylin-Eosin (HE) staining

IVD was sliced longitudinally and half of the disc was fixed in 3.7% PFA, washed in PBS and stored at 4°C. Subsequently, the fragments were placed into histology cassettes, embedded in paraffin wax, cut into 2–4 μm sections and mounted on glass slides (microscopic slides; MGF-slides), previously silanized with a 3-aminopropyltriethoxysilane treatment. Then, paraffin slices were immersed three times

in xylene to remove paraffin, and then re-hydrated using decreasing concentrations of alcohol (twice in 100, 96, 70 and 50%) followed by distilled water. Next, IVD sections were incubated in Gill's haematoxylin (Sigma-Aldrich) for 3 min to stain the cell nuclei. After washing in tap water and dehydrating through graded alcohol solutions (50, 70 and 96%, 3 min each), a counterstaining was performed in alcoholic eosin (Surgipath) for 1 min, to detect cell cytoplasm and most connective tissue fibres. After three quick passages in absolute alcohol and clearing in xylene, the slides were mounted with resinous mounting medium (Quick-D; Klinipath).

2.10 NP Safranin O-Light green staining

sGAG deposition was analysed by Safranin O-Light green staining of NP tissue. Paraffin-embedded IVD sections were incubated in Gill's haematoxylin (Sigma-Aldrich) for 5 min to stain the cell nuclei. After washing in distilled water for 15 s, the samples were immersed in 0.4% Light green (Sigma) solution during 5 min to stain the cytoplasm. Following two washes (of 3 min each) in 1% acetic acid solution, slices were immersed for 4 min in 0.1% Safranin O (Sigma-Aldrich) solution to detect sGAG deposition. Then, samples were dehydrated through graded alcohol solutions (three quick dips in 96% and three times in 100% for 3 s each) and cleared in xylene. Finally, slides were mounted with resinous mounting medium (Quick-D, Klinipath).

2.11 Metabolic activity of IVD organotypic cultures

Metabolic activity was evaluated through the resazurin assay that measures the bioreduction of resazurin to resorufin, which can be detected using fluorescence (530/590 nm). To analyse metabolic activity of IVD organ cultures treated with the different solutions, the CEPs of each IVD in culture were removed using a scalpel. Each IVD was cut sagittally in half (comprising AF and NP) and incubated in 8 mL of cell culture medium containing 10% resazurin solution (0.1 mg/mL resazurin sodium salt ($C_{12}H_6NNaO_4$, Sigma) in PBS) for 3 h at 37°C, to guarantee linearity between IVD weight and resazurin conversion (Supplementary Fig. S2 compared results of 1 IVD comprising AF, NP and CEPs, 1 IVD without CEPs, plus $\frac{3}{4}$ IVD, $\frac{1}{2}$ IVD and $\frac{1}{4}$ IVD also with AF and NP tissue. Results showed that the IVD metabolic activity correlates with tissue wet weight from 0 to 2.6 g, or tissue dry weight from 0 to 0.3 g, corresponding to $\frac{3}{4}$ IVD tissue). A blank control comprising only medium was also included. For each experimental condition, three independent donors were selected. Metabolic cell activity was expressed as relative fluorescent units and normalised to the tissue wet weight.

2.12 DNA quantification of IVD organotypic cultures

To quantify DNA content, frozen NP was minced into very small pieces with the help of tweezers and a scalpel. After freeze-drying, the samples were digested overnight at 56°C with proteinase K (0.5 mg/mL in phosphate buffer containing 10.68 g/L $NaH_2PO_4 \cdot 2H_2O$, 8.45 g/L $Na_2HPO_4 \cdot 7H_2O$ and 3.36 g/L disodium-EDTA in ultrapure water) [57]. pH was previously adjusted to 6.5. After vortexing and centrifugation, the cellularity of each sample was measured based on the DNA content using a CyQuant® kit (Invitrogen) with lambda DNA as a standard. DNA content was expressed as relative fluorescent units and normalised to the tissue dry weight (Supplementary Fig. S3). For each experimental condition, three independent donors were selected.

2.13 sGAG quantification in IVD organotypic cultures

sGAG content of IVD organotypic cultures was analysed on NP tissue by reaction with 1,9-Dimethyl-Methylene Blue zinc chloride double salt (DMMB; Sigma-Aldrich) dye reagent solution, containing 40 mM sodium chloride (NaCl; Roth), 40 mM Glycine (Roth) and 46 μ M DMMB, previously adjusted to pH 3.0. Chondroitin sulphate A sodium salt from bovine trachea (Sigma) was used as standard. Results were normalised to the corresponding DNA content, quantified as previously described. For each experimental condition, three independent donors were selected.

2.14 Free active TGF- β 1 quantification

TGF- β 1 concentration in IVD organotypic culture supernatants was analysed by ELISA (LEGEND MAX™ Free Active TGF- β 1 ELISA Kit, BioLegend®), according to the manufacturer's instructions. Results were normalised to the DNA content of NP tissue. Three independent donors were selected.

2.15 Detection of Col II in the NP

Col II deposition in NP tissue was analysed by immunofluorescence (IF) staining and western blot analysis. For IF, antigen retrieval was performed in paraffin-embedded IVD slices through incubation with a 20 μ g/mL proteinase K (Sigma-Aldrich) solution for 15 min at 37°C. A blocking step was introduced to reduce non-specific background staining with 1 h incubation in PBS containing 1% bovine serum albumin (BSA; Sigma-Aldrich) and 0.1% Triton X-100 (Sigma). Sections were then incubated for 2 h at 37°C with mouse anti-Col II (1 : 50) in the dark (monoclonal antibody (II-II6B3) developed by Dr. Thomas F.

Linsenmayer, from the Developmental Studies Hybridoma Bank under the auspices of the NICHD and maintained at the University of Iowa, Department of Biology, Iowa City, IA, U.S.A.). A fluorescent secondary antibody (Invitrogen) was diluted 1:1000 and incubated during 1 h. After washing in PBS, the samples were mounted in Fluoroshield mounting medium with DAPI (Sigma). As positive controls, human nasal cartilage sections were used, while samples without primary antibody were chosen as negative controls.

Col II detection was also performed by western blot analysis using the same antibody. Frozen NP was minced into very small pieces with the help of tweezers and a scalpel. Proteins were extracted in a buffer containing 4 M guanidine hydrochloride (Sigma), 3 M sodium acetate (Merck) and 10 mM ethylenediaminetetraacetic acid (EDTA; Sigma-Aldrich), and enriched with 1 mM of phenylmethylsulfonyl fluoride (PMSF; Sigma), a protease and phosphatase inhibitor cocktail (Roche Diagnostics GmbH and Sigma, respectively) and 65 mM of freshly added dithiothreitol (DTT; Sigma) for 24 h at 4°C. Following centrifugation, ethanol precipitation and ressolubilization, proteins were quantified using 2-D Quant Kit (GE Healthcare) according to the manufacturer's instructions. Protein samples (15 µg) were separated by sodium dodecyl sulphate (SDS)/9% polyacrylamide gel electrophoresis, and electroblotted onto a Hybond enhanced chemiluminescence (ECL) membrane (Amersham Biosciences/GE Healthcare). After incubation with the monoclonal antibody against Col II (1:2000), an anti-mouse (1:3000; Amersham Biosciences) horseradish peroxidase-conjugated secondary antibody was used. Then, ECL detection (Amersham Biosciences) was performed. Bands were quantified using Quantity One® 4.6.6 Software (Bio-Rad, Amadora, Portugal). Values were normalised to the density of each corresponding lane, following brief membrane staining with PageBlue-Coomassie Brilliant Blue G-250, Thermo Scientific) and by Col II expression levels of the control (fresh IVDs). Three independent donors were selected.

2.16 Statistical analysis

Statistical analysis was performed using GraphPad Prism (version: 5.0a). The parametric distribution of the data was first evaluated by D'Agostino & Pearson omnibus normality test. Since the data followed a non-parametric distribution, statistical analysis was performed by the Friedman test followed by the Dunn's multiple comparison post-test to compare more than 2 groups of paired samples. The Kruskal-Wallis test was used to compare more than two groups of unpaired samples. A confidence interval of at least 95% was chosen to define statistical significance (* $p < 0.05$, ** $p < 0.025$, *** $p < 0.001$).

3 Results

3.1 Characterisation of γ -PGA/Ch NCs at pH 5.0 and pH 7.4

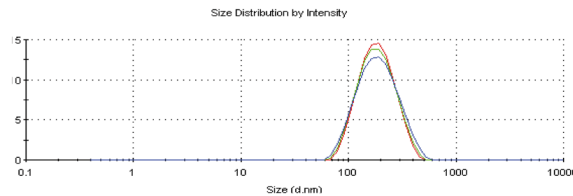
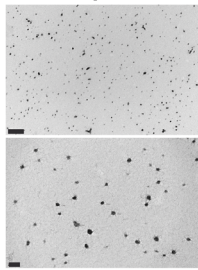
γ -PGA/Ch NCs were first prepared at pH 5.0, as previously reported [55]. To obtain γ -PGA/Ch NCs at physiological pH (with similar polymers concentration), NCs at pH 5.0 were concentrated in an acidic-buffered solution, and diluted in cell culture medium at pH 7.4. The comparison of NC features at both pHs is summarised in Fig. 3.

NCs obtained by complex coacervation at pH 5.0 resulted in spherical particles with occasional clusters of 2–3 individual NCs ($d = 238.2 \pm 39.1$ nm). They presented a relatively monodisperse size distribution (PDI = 0.3 ± 0.0) with a ζ potential of 20.3 ± 0.5 mV (Fig. 3a). γ -PGA/Ch NCs were centrifuged and concentrated. Analysis of the resulting NC supernatant confirmed a low frequency of events with a size smaller than that of NCs, but also in a monomodal distribution. NCs were identified in the pellet resulting from centrifugation, with increased concentration, and in a homogeneous population, with identical ζ potential, confirming the success of NCs centrifugation step (Supplementary Fig. S1a and S1b). In turn, concentrated NCs diluted in cell culture medium (pH 7.4) resulted in a highly disperse size distribution (PDI = 0.9 ± 0.1) (Fig. 3b). And so, particles with three different sizes could be distinguished: the majority ($61.1 \pm 1.6\%$) with bigger size (767.2 ± 249.6 nm), and two other groups in lower percentages (27.1 ± 0.9 and $11.1 \pm 1.2\%$) and lower sizes (11.6 ± 1.7 and 30.7 ± 1.3 nm, respectively). The number of total events detected was also smaller than those of Fig. 3a (NCs directly obtained from the complex coacervation method), 119.9 ± 2.6 kcps, and with a slightly negative average ζ potential (-9.4 ± 0.5 mV) (Fig. 3b). Cell culture medium alone was also analysed and small particles (13.3 ± 0.5 nm) were also identified, similarly to what was observed with NCs at pH 7.4 (Supplementary Fig. S1c).

Concerning NCs morphology, NCs presented a spherical shape in acidic pH, with the denser material (black) appearing to constitute the majority of the NCs, particularly their core. At pH 7.4, large aggregates of dense material were easily distinguished, with a less dense material surrounding them in an irregular and disperse manner. Still, the morphology of NCs at pH 5.0 (Fig. 3a) was not clearly detected at pH 7.4 (Fig. 3b).

3.2 Quantification of γ -PGA/ftCh NC internalisation by NP cells

γ -PGA/Ch NCs' internalisation within NP cells was assessed through Ch labelling (ftCh) and further incubation of the γ -PGA/ftCh NCs with NP cells. By standard flow

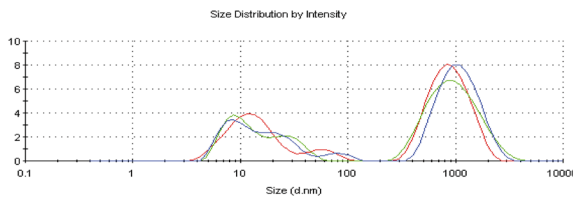
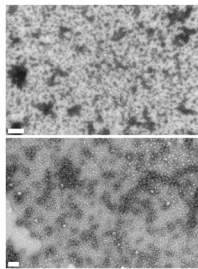
γ -PGA/Ch NCs**(a) NCs at pH 5.0**

$$d_{PK1}: 238.2 \pm 39.1 \text{ nm (100\%)}$$

$$Pdl: 0.3 \pm 0.0$$

$$\zeta \text{ pot.}: 20.3 \pm 0.5 \text{ mV}$$

$$mcr: 212.1 \pm 36.6 \text{ kcps}$$

(b) NCs at pH 7.4

$$d_{PK1}: 767.2 \pm 249.6.6 \text{ nm (61.1} \pm 1.6\%)$$

$$d_{PK2}: 11.6 \pm 1.7 \text{ nm (27.1} \pm 0.9\%)$$

$$d_{PK3}: 30.7 \pm 5.3 \text{ nm (11.1} \pm 1.2\%)$$

$$Pdl: 0.9 \pm 0.1$$

$$\zeta \text{ pot.}: -9.4 \pm 0.5 \text{ mV}$$

$$mcr: 119.9 \pm 2.6 \text{ kcps}$$

Fig. 3 Characterisation of γ -PGA/Ch NCs. NCs were characterised immediately after preparation in 0.05 M Tris-HCl with 0.15 M NaCl buffer at pH 5.0 **a** and after incubation in cell culture medium (high-glucose Dulbecco's Modified Eagle Medium (DMEM) supplemented with 2% Fetal Bovine Serum (FBS), 1% penicillin/streptomycin (P/S), 1% Insulin-Transferrin-Selenium (ITS) supplement and 0.1% Fungizone (Amphotericin B)) at pH 7.4 **b** ($n=3$). Size (d, nm),

polydispersity index (Pdl), ζ potential (ζ pot., mV) and mean count rate (mcr, Kcps) measurements, determined by dynamic and electrophoretic light scattering (DLS and ELS), were displayed for each step, together with particle size distribution plots obtained by intensity of the scattered light (using the same equipment) and representative transmission electron microscope (TEM) images (bars represent 500 and 100 nm, respectively) (color figure online)

cytometry, 91.1% of the NP cells presented ftNCs (Fig. 4a). However, with this technique NC internalisation is not distinguishable from NC presence in the cell membrane. Therefore, NC internalisation was further assessed using image flow cytometry. With this technique it was possible to observe that from the 63.0% of NP cells with ftNCs (Fig. 4b), 34.9% (approximately 22% of total NP cells) presented higher fluorescence intensity inside the cell (R3 group), being the NCs effectively internalised, and approximately 62.6% of these cells presented NCs only associated with the cell membrane (R5 group) (Fig. 4c).

3.3 Impact of γ -PGA and γ -PGA/Ch NCs at different pHs (pH 5.0 and pH 7.4) on tissue architecture, metabolic activity and DNA content of ex vivo IVD organotypic cultures

The first impact of γ -PGA and γ -PGA/Ch NC treatments was evaluated in ex vivo IVD organotypic cultures after 2 days in culture. The general architecture of the NP central region, next to the cavity created, was visualised using HE histological staining (Fig. 5). An extensive presence of extracellular matrix (ECM) was clearly distinguished within fresh IVDs. The matrix contained some diffuse flashes of

lighter eosinophilia, along with a low cell density. All cells presented a round-shaped morphology with lacunae formation (chondrocytic cells). The majority of the cells were found in 2-cell clusters, but larger groups of cells in close proximity were also frequently observed. In IVDs with cavity, other differences were detected: thin basic fibres could be perceived in some areas of the NP core through the eosin staining. The majority of the cells presented a round-shaped morphology, but some cells had a more elongated shape. Some 2-cell clusters were found within the matrix, along with single cells.

With acidic solutions' (solvent or γ -PGA/Ch NCs, at pH 5.0) injection, the NPs' ECM appeared to be sparse: diffusely distributed shades of pale pink could be seen and fewer cells were present. Some cells appeared more elongated, while others seemed smaller and with an irregularly shaped cytoplasm, contrarily those seen with the other conditions. Most cells were found isolated and 2-cell clusters were rarely observed. When NCs were included, intensely stained bundles of basic fibrillar structures appeared arranged as a network. Cells, which displayed chondrocyte-like features with prominent lacunae, were mostly placed between those fibres. On the other hand, at pH 7.4 (solvent, γ -PGA/Ch NCs or γ -PGA, at pH 7.4), NP ECM seemed to

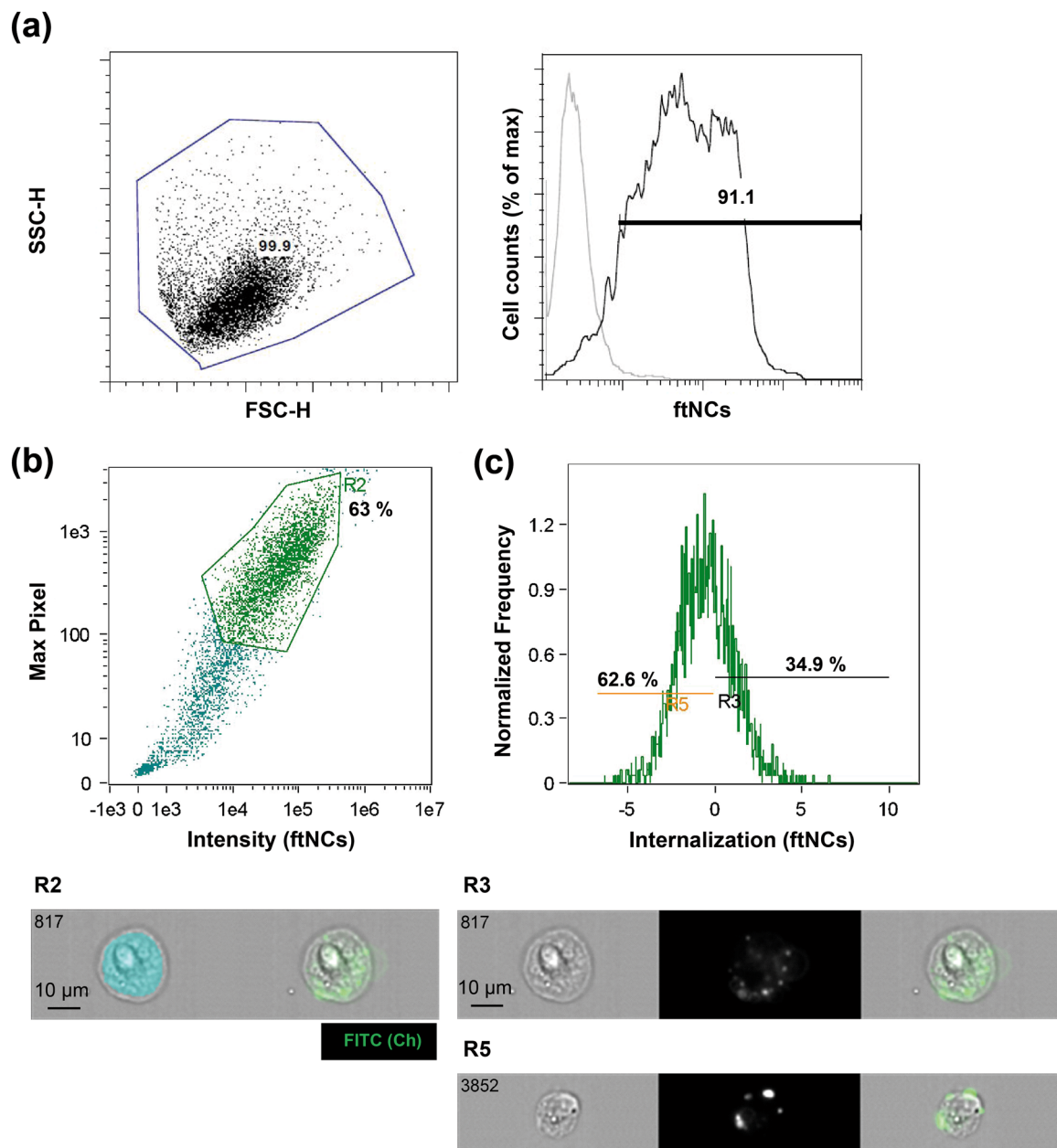


Fig. 4 Flow cytometry analysis of fluorescent γ -PGA/Ch NCs (ftNCs) internalization by isolated bovine IVD cells from a pool of 6 discs. **a** Dot plot and histogram profiles for the ftNCs internalisation analysis by standard flow cytometry. **b** Dot plot profiles for the ftNCs internalisation analysis by imaging flow cytometry. **c** Histogram profile,

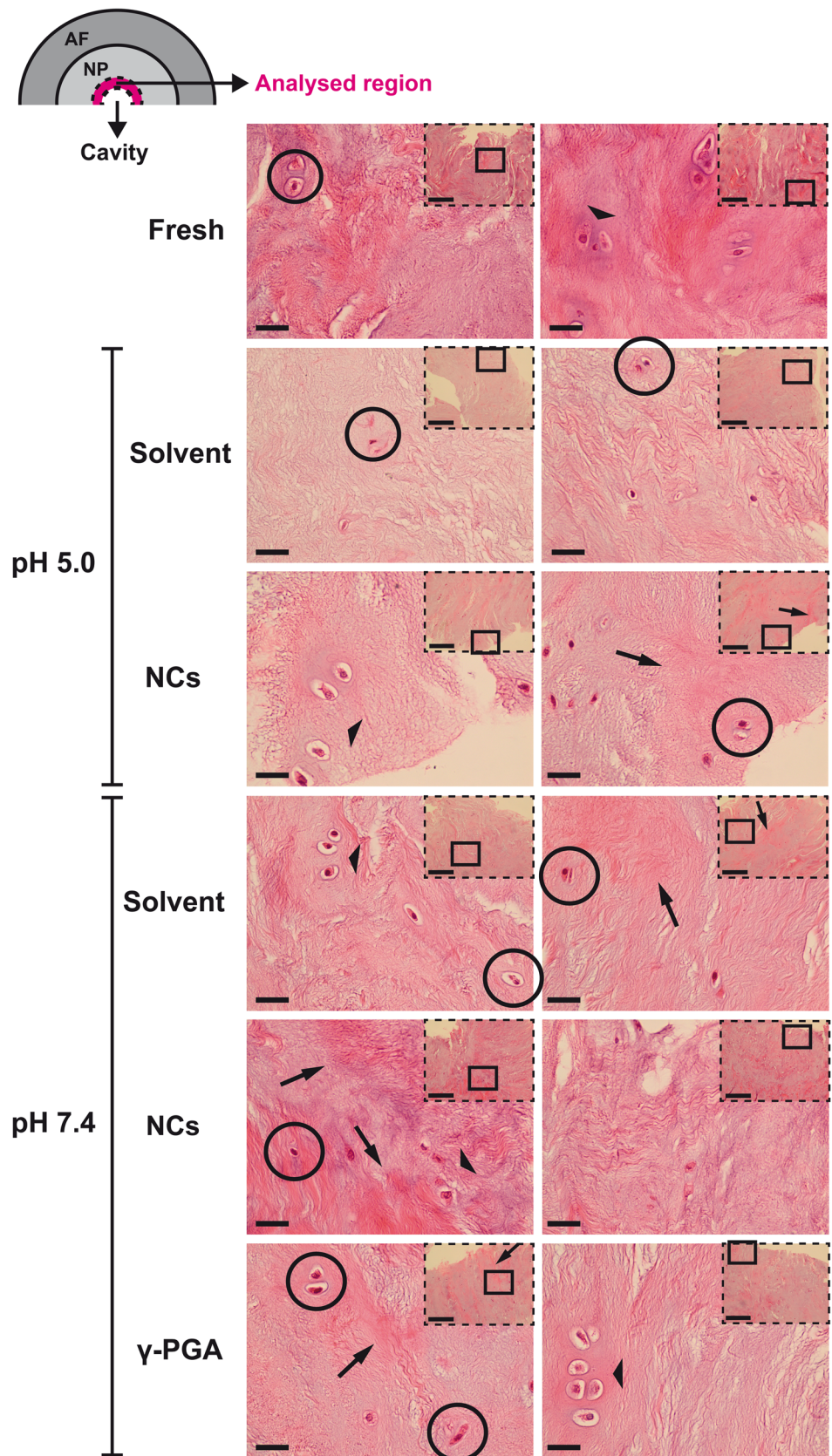
after application of an internalisation mask, showing cells negative (R5) and positive (R3) for ftNCs internalisation. Each cell is represented by a row of three images acquired simultaneously in flow - from left to right: brightfield (grey), FITC fluorescence (green) from the NCs, merged image (color figure online)

be more organised. More intense bundles of eosinophilic ECM appeared to be observed in IVDs treated with NCs and γ -PGA. With NCs, the ECM looked more heterogeneous, with a few large acidophilic areas next to densely packed fibre bundles oriented as networks. In turn, with γ -PGA, the oriented structures were the dominant feature. At the cellular level, the main differences at this pH were occasional double-eyed chondrocytes sharing the same

territorial matrix and several groups with more than 3 cells in close proximity.

Metabolic activity and DNA content of organotypic cultures, when in contact with solvent, γ -PGA or γ -PGA/Ch NCs were also assessed after 2 days in culture (Fig. 6). Both acidic conditions—solvent ($*p < 0.05$) or γ -PGA/Ch NCs ($**p < 0.025$), at pH 5.0 - led to a reduced metabolic activity of IVD cells when compared with fresh IVDs.

Fig. 5 NP architecture of NP from IVDs after 2 days in culture, obtained by haematoxylin/eosin histological staining. A fresh IVD was compared with IVDs with cavities filled with: γ -PGA/Ch NCs at pH 5.0 and pH 7.4 (NCs), the respective solvents, and γ -PGA. One representative donor is presented. Columns give detailed images of distinct regions of each NP centre (bars represent 25 μ m). Inserts represent general overviews over the latter regions (bars represent 500 μ m). Cells are highlighted with black circles (occasional elongated cells; singular round-shaped cells with lacunae formation, double-eyed or 2-cell clusters) and black large arrowheads (groups of 3-8 round-shaped cells). The black thinner arrows highlight intense basic extracellular fibres (color figure online)



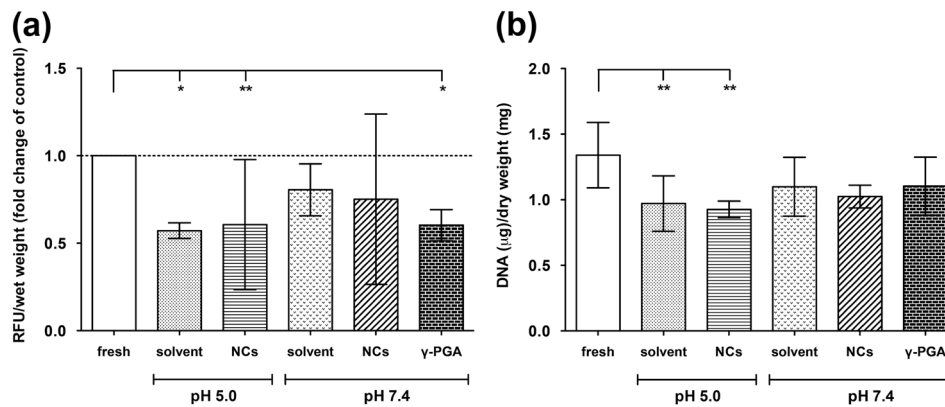


Fig. 6 **a** Metabolic activity of IVD organ cultures in the presence of γ -PGA and γ -PGA/Ch NCs after 2 days **b** NP DNA content of IVD organ cultures in the distinct settings after 2 days. The following groups were compared: fresh, solvent at pH 5.0 (0.05 M Tris-HCl with 0.15 M NaCl buffer) and γ -PGA/Ch NCs prepared in the buffered solution (NCs), and at pH 7.4: solvent (cell culture medium), solvent supplemented

with γ -PGA/Ch NCs (NCs), or with γ -PGA. Results are shown as mean \pm SD from three independent donors. Statistical significance was considered for at least $*p < 0.05$, $**p < 0.025$, $***p < 0.001$, using the Friedman paired test followed by the Dunn's multiple comparison post-test

When γ -PGA/Ch NCs were injected at pH 7.4, in cell culture medium, this effect was not observed, although γ -PGA injection at physiological pH also resulted significant metabolic activity decrease ($*p < 0.05$), as observed with acidic conditions.

NP DNA content was also analysed and its reduction was more evident when acidic solutions were injected into the IVD ($**p < 0.025$), in comparison with solutions at physiological pH (Fig. 6b). DNA content normalisation by dry weight was selected since the water content is the higher contributor to NP's weight. So, small variations in NP tissue sampling can result in pieces of tissue with different water retention capacity, and a higher error associated with this normalisation (Supplementary Fig. S3). Thus, although IVD wet weight is widely used in the literature as a measure of IVD size or cell number [60–64], it is not the most accurate method for normalisation, since small variations in the water content of this tissue (that can be related to different IVD sizes, different region within the tissue(s), etc.) can have a pronounced effect on IVD wet weight.

In this study, the quantification of IVD cell metabolic activity could not be directly related with DNA content, since the former was analysed in an IVD fragment comprising both AF and NP, while DNA was quantified in the NP tissue near the cavity region of each IVD.

3.4 Impact of γ -PGA and γ -PGA/Ch NCs, at pH 7.4, on the ECM of ex vivo IVD organotypic cultures

To evaluate if NCs could have an impact on the production of cartilaginous matrix deposition in the IVDs with time, organ cultures were extended to 7 days. Since γ -PGA/Ch NCs at pH 7.4 had a significantly lower impact on tissue

viability, only studies conducted at this pH were carried out and compared to the solvent at pH 7.4.

After 7 days in culture, a small increase in the DNA content of IVDs cultured with γ -PGA/Ch NCs and γ -PGA could be observed, although not statistically significant (Fig. 7a). Furthermore, the sGAGs of IVDs cultured with γ -PGA seemed to be more uniformly distributed throughout the IVD sections and in higher amounts than at day 2 (Figs. 7b and 7c). This observation was made after comparison with fresh IVDs. The possible interference of γ -PGA in the process of sGAG staining was discarded, after analysing AF from the same tissue sections and confirming that no red/orange staining was observed in neither of the samples (Supplementary Fig. S4). Endogenous free active TGF- β 1 was quantified in culture supernatants (Fig. 6d), since TGF- β 1 is known to inhibit matrix degradation, being associated with higher NP cell proliferation [65, 66], PG synthesis [16, 67] and Col II production when supplemented to the culture medium [68]. However, although slightly higher values were detected in the presence of γ -PGA after 7 days in culture, no statistical differences were observed between the conditions under study.

Col II distribution within IVD organ cultures was assessed by IF during 2 and 7 days and its production quantified by western blot analysis after day 7. To compare the different conditions, image acquisition settings were maintained among the different samples (Fig. 8a). Col II labelling (red) appeared to be enhanced with γ -PGA and NC treatments, in respect to the corresponding solvent controls. Nevertheless, some heterogeneity (particularly with NCs) was displayed in regard to Col II distribution and intensity. Col II was also quantified by western blot, after 7 days in culture by western blot (Fig. 8b). When compared with fresh IVDs, a significant decrease ($*p < 0.05$) in Col II

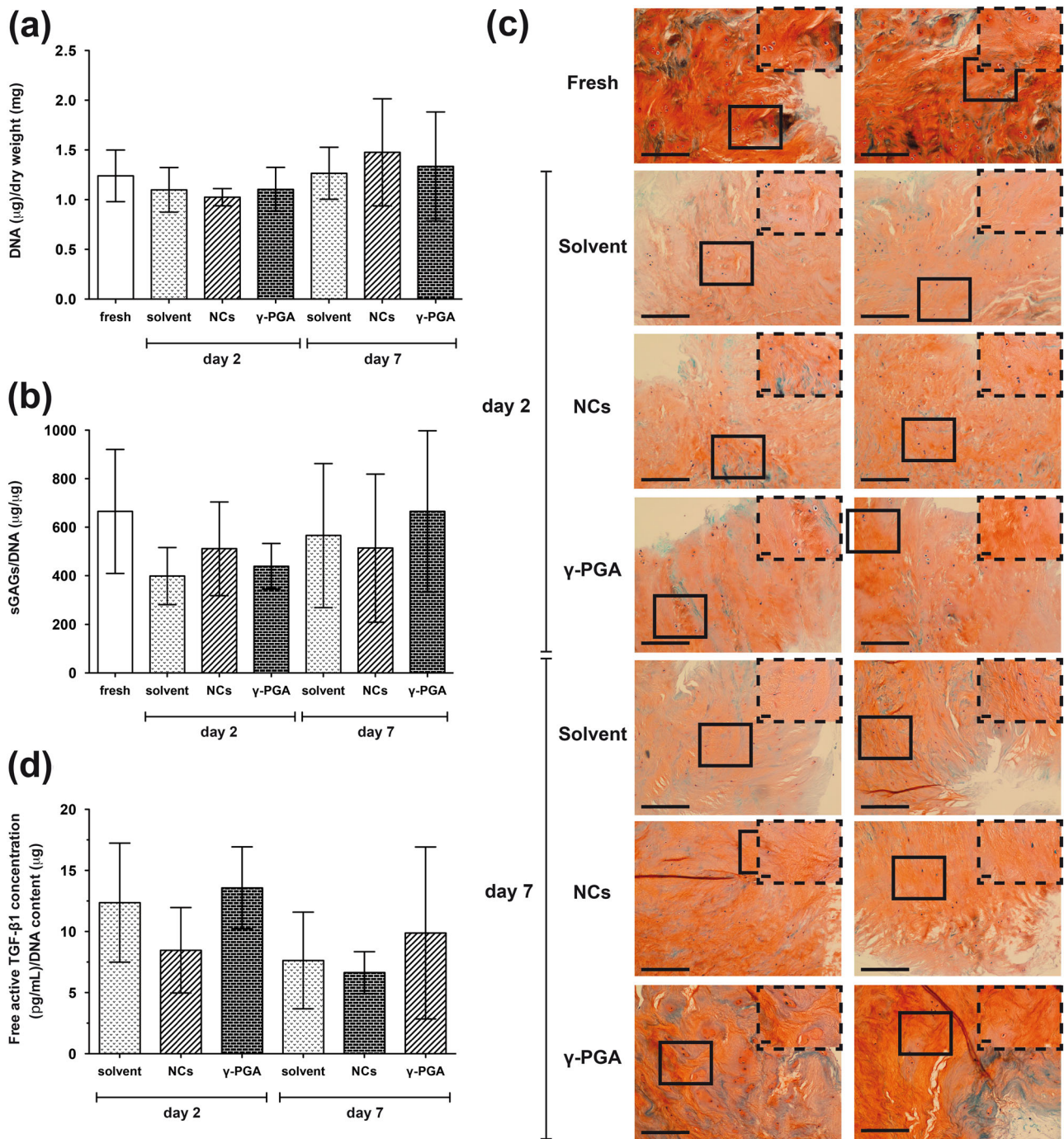


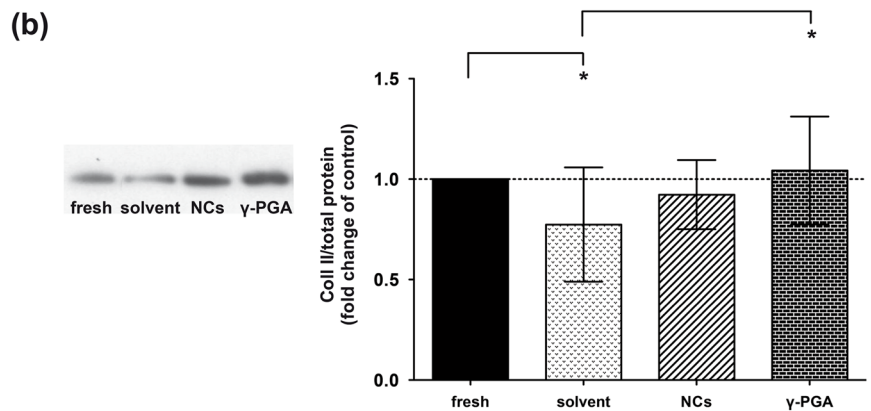
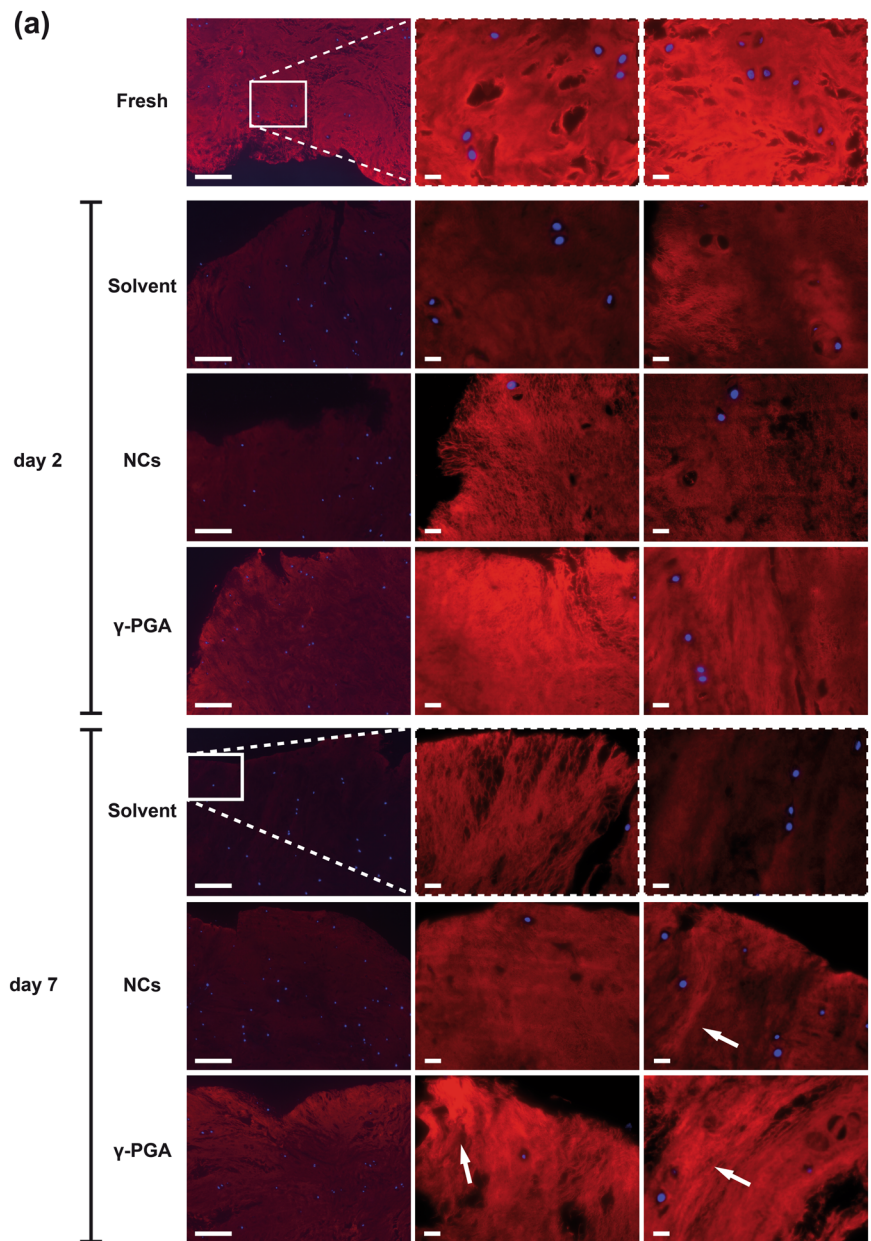
Fig. 7 Evaluation of ECM synthesis of IVD organ cultures in the presence of γ -PGA and γ -PGA/Ch NCs at pH 7.4 during 7 days of culture. **a** DNA content of NP tissue; sGAG deposition **b** and distribution **c** (*Safranin O*/*Light green* histological staining). Representative donors are presented here. Columns give general overviews over distinct regions of each NP centre (bars represent 500 μ m); inserts represent detailed images of the latter regions (bars represent 25 μ m). **d**

Free active transforming growth factor beta 1 (TGF- β 1) concentration in culture supernatants. **a**, **c** and **d** Results are represented as mean \pm SD from three independent donors/time point. Statistical significance was considered for at least $*p < 0.05$, $**p < 0.025$, $***p < 0.001$, using the Kruskal-Wallis test followed by the Dunn's multiple comparison post-test (color figure online)

content could be observed in IVDs treated with solvent alone. For IVDs cultured in the presence of γ -PGA/Ch NCs, a recovery of Col II to levels close to those of freshly isolated IVDs was observed. On the other hand, a clear

significant augment of Col II content was reached with γ -PGA-treated IVDs ($*p < 0.05$) in detriment of the solvent treatment.

Fig. 8 Distribution (red) **a** and quantification **b** of type II collagen (Col II) deposition (red) in NP tissue cultured for 7 days in culture with different treatments at pH 7.4: cell culture medium (solvent), solvent supplemented with γ -PGA/Ch NCs (NCs), or with γ -PGA. First column contains low magnification images (bars represent 250 μ m). The 2 columns to the right are detailed images of distinct areas of the cavity region (bars represent 25 μ m). White arrows point to more intense Col II fibre bundles. IVDs from representative donors are presented here. For Col II quantification the results are represented as mean \pm SD from three independent donors. Statistical significance was considered for at least $*p < 0.05$, ($**p < 0.025$, $***p < 0.001$), using the Friedman paired test followed by the Dunn's multiple comparison post-test. A representative immunoblot is shown (color figure online)



4 Discussion

This study addresses the application of γ -PGA or γ -PGA/Ch NCs to IVD regeneration. Recently, our group has shown that γ -PGA increases and accelerates cartilaginous ECM production in MSC pellet in vitro cultures when used as a supplement in cell culture medium [30]. Herein, γ -PGA/Ch NCs, previously developed by our group [55], were also tested as a supplement in cell culture medium while injected directly into the cavity, an approach that promotes the closest contact possible with the damaged tissue. Hence, NCs were tested in the cell culture medium at pH 7.4. Notwithstanding, NCs were additionally evaluated in the solvent in which they were built - the aforementioned buffered solution at pH 5.0 - to be able to infer on their impact on degenerated IVDs.

Stable polyelectrolyte NCs were produced through electrostatic interactions promoted by an acidic pH, as previously described [54, 55]. Positive charge and TEM analysis suggest that the protonated Ch, the larger polyion, has a major contribution for polymers' assembly (as suggested by Lin and colleagues [69]). To inject NCs at physiological pH, these were concentrated by centrifugation and resuspended in cell culture medium, at pH 7.4. Nevertheless, NCs' dilution in the cell culture medium resulted in a higher polydispersed size distribution, in which the major contribution to the detected events came from larger compositions that indicated swelling and/or agglomeration of NCs. Particle agglomeration and swelling have already been reported by Hadju et al. [70]. This was expected due to deprotonation of the amine groups of Ch amine groups and γ -PGA chain expansion at neutral pH [70].

Both γ -PGA and γ -PGA/Ch NCs at pH 5.0 and 7.4 were injected in a nucleotomised IVD ex vivo culture model [56, 57, 60]. Injection of Ch alone was not explored in this study, since this polymer is not soluble at physiological pH [71]. Moreover, being Ch the only naturally occurring cationic GAG analogue [72–75], it has already been widely described for cartilage [75–77] and IVD [78–82] regeneration.

It is known that organ cultures provide a more physiological environment than in vitro conditions, in this case maintaining IVD cells in a microenvironment closer to that of an in vivo scenario (hypoxia, limited nutrition, etc.) [83–85]. The bovine model was selected due to having anatomic proportions close to the human IVD, similar matrix composition, cell phenotype and nutrient transport [83, 86]. IVDs injected with solutions at pH 5.0, particularly the solvent alone, showed the presence of cells with an irregular cytoplasm within the NP centre (possibly necrotic cells). On the other hand, the IVDs with solutions at pH 7.4 presented more cells and a denser matrix. These cells presented

typical chondrocyte morphology and banded basic fibrillar structures (stained in pink). Such staining is related with positively charged structures like cationic amine groups of Col, suggesting the existence of a Col network [3, 4, 10]. Ch itself could also take part in these networks, as defended by Roughley et al. [82].

Previous studies by our group have shown no cytotoxicity of γ -PGA and γ -PGA/Ch PECs on human MSCs/chondrocytes [30] and fibroblasts/macrophages [54, 58] cultures, respectively. Herein, no major cytotoxicity was observed in IVD, although a decline in bovine NP cell metabolic activity has been reported by pH reduction to 6.2 within 24 h of in vitro culture, particularly under nutrient deficit conditions (low oxygen and low glucose concentrations) [87]. γ -PGA/Ch NCs were shown to be internalised by NP cells, although we cannot exclude that the biological effect of these NCs could be due to interaction with membrane receptors, as suggested by other works [40, 88–90]. In this work, imaging flow cytometry technique was used due to its potential as a high throughput method compared with standard flow cytometry (which fails to accurately quantify internalised vs. cell bound particles due to low resolution [54]), and regular fluorescence microscopy (as shown by Phanse et al. [91] for cellular internalisation of nanoparticles).

A significant reduction in DNA content of IVDs treated with NCs at pH 5.0 was also observed. However, at pH 7.4 this effect was not observed for all the solutions tested (solvent, γ -PGA/Ch NCs or γ -PGA).

In light of the results obtained, given that it is known that bovine NP cells do not survive in vitro at pH 6.0 for more than 12 days [92, 93], show detrimental features (water loss, elevated intracellular ionic strength, subsequent cell shrinkage with physical distortion of the nuclear matrix and cytoskeleton disorganisation [94], reduction of NP cell ability to synthesise novel DNA [94, 95], increase of cell senescence and decrease of cell viability [96–99]) after exposure to high salt concentrations (as with the Tris-HCl with NaCl buffer solution), only the effect of γ -PGA and γ -PGA/Ch NCs in the solvent at pH 7.4 was investigated in IVD ECM after 7 days in culture. Moreover, since increased cartilaginous matrix formation could be observed in MSC pellet in vitro cultures in which γ -PGA-supplemented cell culture medium was used [30], the chosen solvent for the present analyses was also cell culture medium, here adapted to IVD organotypic cultures. The latter solvent has been considered an ideal solution to maintain cell viability, ensure the feasibility of whole-organ ex vivo cultures and rely on the results obtained [56, 57, 100, 101]. An improvement to its effect would be an achievement worth exploring. Notwithstanding, the previous treatments were not all compared at this time point also due to the limited availability of IVDs from the same bovine tail.

Interestingly, at pH 7.4, an increase in PG staining was observed in the presence of γ -PGA and an evident augment in Col II synthesis was detected in the presence of both γ -PGA and γ -PGA/Ch NCs, but particularly with γ -PGA treatment. These results show that γ -PGA, besides promoting Col II production by human MSCs [30], can have a similar effect in the NP. Of notice, all the outputs obtained in this study were analysed at the protein-level; an added value compared with most IVD studies that only show outputs at gene expression level [57, 61, 102]. Although the specific mechanism of action of γ -PGA remains to be investigated, we hypothesise that the glutamate pool generated upon γ -PGA biodegradation may activate the glutamate signalling pathway [103]. Glutamate signalling is known to modulate chondrocyte proliferation [104] and their response to mechanical stimulation [105]. Despite the fact that no specific data has been reported for Ch's mechanism of action in IVD cells, other polysaccharides (of herbal origin [106, 107]) have been shown to promote rat chondrocyte proliferation [106, 107] and increase Col II expression [107] through the Wnt/ β -catenin signalling pathway. On the other hand, Peng and colleagues [88] have shown that γ -PGA/Ch NCs are internalised by human fibrosarcoma cells (HT1080) via non-specific charge-mediated interaction between the NCs (positively charged) and the cell membrane components (negatively charged proteoglycans via a specific protein-mediated endocytosis).

Moreover, both γ -PGA solution and γ -PGA/Ch NC dispersion are liquid solutions and easy to inject. This is an advantage compared with highly viscous hydrogel solutions. Although we cannot exclude the risk of leakage, a beneficial effect was observed with these solutions, using a single-dose injection. Therefore, this effect could be further explored by evaluating multiple injections, different polymer/NC concentrations and biomolecules' delivery, among others.

5 Conclusions

The application of γ -PGA and γ -PGA/Ch NCs on nucleotomised IVD was screened for the first time. γ -PGA/Ch NC injection at acidic pH was detrimental to IVD organ cultures, decreasing the DNA content of the tissue(s). Nevertheless, these effects were overcome by NC injection at pH 7.4. In this condition, γ -PGA alone and γ -PGA/Ch NCs were able to promote Col II production after 7 days in culture. This study is the first proof of concept that γ -PGA-based injections can be used in a degenerated IVD context. Promising outcomes can be perceived for the future use of γ -PGA-based strategies in its soluble form or in the form of NCs that may additionally deliver biologically active molecules into the IVD.

Acknowledgments This work was financed by FEDER funds through the Programa Operacional Factores de Competitividade—COMPETE, by Portuguese funds through FCT—Fundação para a Ciência e a Tecnologia in the framework of the project PEst-C/SAU/LA0002/2011. Catarina Leite Pereira and Graciosa Teixeira are grateful to FCT for their Ph.D. grants (SFRH/BD/85779/2012, SFRH/BD/88429/2012) and Joana Caldeira for her Post-Doc grant (SFRH/BPD/78187/2011). Raquel M. Gonçalves is also grateful to FCT for FCT Investigator Starting Grant (IF/000638/2014). The authors would also like to thank to Maria Molinos, Carla Cunha, Juliana Alves, António Ribeiro and Susana Carrilho for technical assistance/guidance during experiments. The authors would also like to acknowledge Carnes Landeiro, S. A. for providing the bovine tails.

Compliance with ethical standards

Conflict of interest The authors declare that they have no competing interests.

References

- 1 An HS, Thonar E, Masuda K. Biological repair of intervertebral disc. *Spine*. 2003;28(15):S86–92.
- 2 Buckwalter JA. Spine update—aging and degeneration of the human intervertebral disc. *Spine*. 1995;20(11):1307–14.
- 3 Smith LJ, Nerurkar NL, Choi K-S, Harfe BD, Elliott DM. Degeneration and regeneration of the intervertebral disc: lessons from development. *Dis Model Mech*. 2011;4(1):31–41.
- 4 Whatley BR, Wen X. Intervertebral disc (IVD): structure, degeneration, repair and regeneration. *Mater Sci Eng C Mater Biol Appl*. 2012;32(2):61–77.
- 5 Chan SCW, Gantenbein-Ritter B. Intervertebral disc regeneration or repair with biomaterials and stem cell therapy—feasible or fiction? *Swiss Med Wkly*. 2012;142:w13598
- 6 Sakai D. Stem cell regeneration of the intervertebral disk. *Orthop Clin North Am*. 2011;42(4):555–62.
- 7 Urban JPG, Roberts S. Degeneration of the intervertebral disc. *Arthritis Res Ther*. 2003;5(3):120–30.
- 8 Boos N, Weissbach S, Rohrbach H, Weiler C, Spratt KF, Nerlich AG. Classification of age-related changes in lumbar intervertebral discs. *Spine*. 2002;27(23):2631–44.
- 9 Adams MA, Roughley PJ. What is intervertebral disc degeneration, and what causes it?. *Spine*. 2006;31(18):2151–61.
- 10 Kuo CK, Li W-J, Tuan RS. Cartilage and ligament tissue engineering: biomaterials, cellular interactions, and regenerative strategies. In: Ratner BD, Hoffman AS, Schoen FJ, Lemons JE, editors. *Biomaterials science: an introduction to materials in medicine*. 3rd ed. Oxford: Academic Press; 2012. p. 1214–36.
- 11 Richardson SM, Freemont AJ, Hoyland JA. Pathogenesis of intervertebral disc degeneration. In: Shapiro IM, Risbud MV, editors. *The intervertebral disc: molecular and structural studies of the disc in health and disease*. Wien: Springer; 2014. pp. 177–200.
- 12 Karppinen J, Shen FH, Luk KDK, Andersson GBJ, Cheung KMC, Samartzis D. Management of degenerative disk disease and chronic low back pain. *Orthop Clin North Am*. 2011;42(4):513–28.
- 13 Schoen FJ. Introduction: rebuilding human using biology and biomaterials. In: Ratner BD, Hoffman AS, Schoen FJ, Lemons JE, editors. *Biomaterials science: an introduction to materials in medicine*. 3rd ed. Oxford: Academic Press; 2012. p. 1119–22.
- 14 Bae WC, Masuda K. Emerging technologies for molecular therapy for intervertebral disk degeneration. *Orthop Clin North Am*. 2011;42(4):585–601.

- 15 Yoon ST, Patel NM. Molecular therapy of the intervertebral disc. *Eur Spine J*. 2006;15:S379–S88.
- 16 Thompson JP, Oegema TR, Bradford DS. Stimulation of mature canine intervertebral-disk by growth factors. *Spine*. 1991;16(3):253–60.
- 17 Walsh AJL, Bradford DS, Lotz JC. In vivo growth factor treatment of degenerated intervertebral discs. *Spine*. 2004;29(2):156–63.
- 18 Akeda K, An HS, Pichika R, Attawia M, Thonar E, Lenz ME, et al. Platelet-rich plasma (PRP) stimulates the extracellular matrix metabolism of porcine nucleus pulposus and annulus fibrosus cells cultured in alginate beads. *Spine*. 2006;31(9):959–66.
- 19 Obata S, Akeda K, Imanishi T, Masuda K, Bae W, Morimoto R, et al. Effect of autologous platelet-rich plasma-releasate on intervertebral disc degeneration in the rabbit annular puncture model: a preclinical study. *Arthritis Res Ther*. 2012;14(6):R241.
- 20 Ilie I, Ilie R, Mocan T, Bartos D, Mocan L. Influence of nanomaterials on stem cell differentiation: designing an appropriate nanobiointerface. *Int J Nanomedicine*. 2012;7:2211–25.
- 21 LaVan DA, McGuire T, Langer R. Small-scale systems for in vivo drug delivery. *Nat Biotechnol*. 2003;21(10):1184–91.
- 22 Müller M, Kessler B, Froehlich J, Poeschla S, Torger B. Polyelectrolyte complex nanoparticles of poly(ethyleneimine) and poly(acrylic acid): preparation and applications. *Polymers*. 2011;3(2):762–78.
- 23 Wang JJ, Zeng ZW, Xiao RZ, Xie T, Zhou GL, Zhan XR, et al. Recent advances of chitosan nanoparticles as drug carriers. *Int J Nanomedicine*. 2011;6:765–74.
- 24 Stuart MAC, Huck WTS, Genzer J, Müller M, Ober C, Stamm M, et al. Emerging applications of stimuli-responsive polymer materials. *Nat Mater*. 2010;9(2):101–13.
- 25 Yang X, Jin L, Yao L, Shen FH, Shimer AL, Li X. Antioxidative nanofullerol prevents intervertebral disk degeneration. *Int J Nanomedicine*. 2014;9:2419–30.
- 26 Liang C-z, Li H, Tao Y-q, Peng L-h, Gao J-q, Wu J-j, et al. Dual release of dexamethasone and TGF-beta 3 from polymeric microspheres for stem cell matrix accumulation in a rat disc degeneration model. *Acta Biomater*. 2013;9(12):9423–33.
- 27 Kandel R, Santerre P, Massicotte E, Hurtig M. Tissue engineering of the intervertebral disc. In: Shapiro I, Risbud M, editors. *The intervertebral disc: molecular and structural studies of the disc in health and disease*. Wien: Springer; 2014. p. 417–33.
- 28 Chang K-Y, Cheng L-W, Ho G-H, Huang Y-P, Lee Y-D. Fabrication and characterization of poly(gamma-glutamic acid)-graft-chondroitin sulfate/polycaprolactone porous scaffolds for cartilage tissue engineering. *Acta Biomater*. 2009;5(6):1937–47.
- 29 Prescott AG, inventor; Crescent Innovations Inc., assignee. *Methods for treating joint pain using poly-gamma-glutamic acid patent US 2006/0234192 A1*. 2006.
- 30 Antunes J, Tsaryk R, Gonçalves R, Pereira C, Landes C, Ghanaati S, et al. Poly(γ -glutamic acid) as an exogenous promoter of chondrogenic differentiation of human mesenchymal stem/stromal cells. *Tissue Eng Part A*. 2015;21:1869–85.
- 31 Liu L-T, Huang B, Li C-Q, Zhuang Y, Wang J, Zhou Y. Characteristics of stem cells derived from the degenerated human intervertebral disc cartilage endplate. *Plos One*. 2011;6(10):e26285
- 32 Risbud MV, Guttapalli A, Tsai T-T, Lee JY, Danielson KG, Vaccaro AR, et al. Evidence for skeletal progenitor cells in the degenerate human intervertebral disc. *Spine*. 2007;32(23):2537–44.
- 33 Blanco JF, Graciani IF, Sanchez-Guijo FM, Muntion S, Hernandez-Campo P, Santamaria C, et al. Isolation and characterization of mesenchymal stromal cells from human degenerated nucleus pulposus comparison with bone marrow mesenchymal stromal cells from the same subjects. *Spine*. 2010;35(26):2259–65.
- 34 Brisby H, Papadimitriou N, Brantsing C, Bergh P, Lindahl A, Henriksson HB. The presence of local mesenchymal progenitor cells in human degenerated intervertebral discs and possibilities to influence these in vitro: a descriptive study in humans. *Stem Cells Dev*. 2013;22(5):804–14.
- 35 Henriksson HB, Thornemo M, Karlsson C, Hagg O, Junevik K, Lindahl A, et al. Identification of cell proliferation zones, progenitor cells and a potential stem cell niche in the intervertebral disc region a study in four species. *Spine*. 2009;34(21):2278–87.
- 36 Sakai D, Nakamura Y, Nakai T, Mishima T, Kato S, Grad S, et al. Exhaustion of nucleus pulposus progenitor cells with ageing and degeneration of the intervertebral disc. *Nat Commun*. 2012;3:1264
- 37 Hellmers F, Ferguson P, Koropatnick J, Krull R, Margaritis A. Characterization and in vitro cytotoxicity of doxorubicin-loaded gamma-polyglutamic acid-chitosan composite nanoparticles. *Biochem Eng J*. 2013;75:72–8.
- 38 Hsieh CY, Tsai SP, Wang DM, Chang YN, Hsieh HJ. Preparation of gamma-PGA/chitosan composite tissue engineering matrices. *Biomaterials*. 2005;26(28):5617–23.
- 39 Kang HS, Park SH, Lee YG, Son TI. Polyelectrolyte complex hydrogel composed of chitosan and poly(gamma-glutamic acid) for biological application: preparation, physical properties, and cytocompatibility. *J Appl Polym Sci*. 2007;103(1):386–94.
- 40 Liao Z-X, Ho L-C, Chen H-L, Peng S-F, Hsiao C-W, Sung H-W. Enhancement of efficiencies of the cellular uptake and gene silencing of chitosan/siRNA complexes via the inclusion of a negatively charged poly(γ -glutamic acid). *Biomaterials*. 2010;31(33):8780–8.
- 41 Tsao CT, Chang CH, Lin YY, Wu MF, Wang JL, Han JL, et al. Antibacterial activity and biocompatibility of a chitosan-gamma-poly(glutamic acid) polyelectrolyte complex hydrogel. *Carbohydr Res*. 2010;345(12):1774–80.
- 42 Chang H-H, Wang Y-L, Chiang Y-C, Chen Y-L, Chuang Y-H, Tsai S-J, et al. A novel chitosan-gamma PGA polyelectrolyte complex hydrogel promotes early new bone formation in the alveolar socket following tooth extraction. *PLoS One*. 2014;9(3):e92362
- 43 Tsao CT, Hang CH, Lin YY, Wu MF, Wang JL, Young TH, et al. Evaluation of chitosan-/poly(glutamic acid) polyelectrolyte complex for wound dressing materials. *Carbohydr Polym*. 2011;84(2):812–9.
- 44 Lin YH, Chen CT, Liang HF, Kulkarni AR, Lee PW, Chen CH, et al. Novel nanoparticles for oral insulin delivery via the paracellular pathway. *Nanotechnology*. 2007;18(10):105102
- 45 Sonaje K, Lin K-J, Wey S-P, Lin C-K, Yeh T-H, Nguyen H-N, et al. Biodistribution, pharmacodynamics and pharmacokinetics of insulin analogues in a rat model: oral delivery using pH-responsive nanoparticles vs. subcutaneous injection. *Biomaterials*. 2010;31(26):6849–58.
- 46 Sonaje K, Lin Y-H, Juang J-H, Wey S-P, Chen C-T, Sung H-W. In vivo evaluation of safety and efficacy of self-assembled nanoparticles for oral insulin delivery. *Biomaterials*. 2009;30(12):2329–39.
- 47 Tang D-W, Hu S-H, Ho Y-C, Mi F-L, Kuo P-L, Sung H-W. Heparinized chitosan/poly(γ -glutamic acid) nanoparticles for multi-functional delivery of fibroblast growth factor and heparin. *Biomaterials*. 2010;31(35):9320–32.
- 48 Tang D-W, Yu S-H, Ho Y-C, Huang B-Q, Tsai G-J, Hsieh H-Y, et al. Characterization of tea catechins-loaded nanoparticles prepared from chitosan and an edible polypeptide. *Food Hydrocoll*. 2013;30(1):33–41.
- 49 Liu Y, Sun Y, Xu Y, Feng H, Fu S, Tang J, et al. Preparation and evaluation of lysozyme-loaded nanoparticles coated with poly-

- gamma-glutamic acid and chitosan. *Int J Biol Macromol.* 2013;59:201–7.
- 50 Hajdu I, Bodnar M, Trencsenyi G, Marian T, Vamosi G, Kollar J, et al. Cancer cell targeting and imaging with biopolymer-based nanodevices. *Int J Pharm.* 2013;441(1-2):234–41.
 - 51 Liao Z-X, Hsiao C-W, Ho Y-C, Chen H-L, Sung H-W. Disulfide bond-conjugated dual PEGylated siRNAs for prolonged multiple gene silencing. *Biomaterials.* 2013;34(28):6930–7.
 - 52 Lin YH, Mi FL, Chen CT, Chang WC, Peng SF, Liang HF, et al. Preparation and characterization of nanoparticles shelled with chitosan for oral insulin delivery. *Biomacromolecules.* 2007;8(1):146–52.
 - 53 Moon H-J, Lee J-S, Talactac MR, Chowdhury MYE, Kim J-H, Park M-E, et al. Mucosal immunization with recombinant influenza hemagglutinin protein and poly gamma-glutamate/chitosan nanoparticles induces protection against highly pathogenic influenza A virus. *Vet Microbiol.* 2012;160(3-4):277–89.
 - 54 Gonçalves RM, Pereira ACL, Pereira IO, Oliveira MJ, Barbosa MA. Macrophages response to chitosan/poly-(gamma-glutamic acid) nanoparticles carrying an anti-inflammatory drug. *J Mater Sci Mat Med.* 2015;26(4):167
 - 55 Pereira CL, Antunes JC, Gonçalves RM, Ferreira-da-Silva F, Barbosa MA. Biosynthesis of highly pure poly-gamma-glutamic acid for biomedical applications. *J Mater Sci Mater Med.* 2012;23(7):1583–91.
 - 56 Pereira CL, Gonçalves RM, Peroglio M, Pattappa G, D'Este M, Eglin D, et al. The effect of hyaluronan-based delivery of stromal cell-derived factor-1 on the recruitment of MSCs in degenerating intervertebral discs. *Biomaterials.* 2014;35(28):8144–53.
 - 57 Peroglio M, Eglin D, Benneker LM, Alini M, Grad S. Thermo-reversible hyaluronan-based hydrogel supports in vitro and ex vivo disc-like differentiation of human mesenchymal stem cells. *Spine J.* 2013;13(11):1627–39.
 - 58 Antunes JC, Pereira CL, Molinos M, Ferreira-da-Silva F, Dessí M, Gloria A, et al. Layer-by-layer self-assembly of chitosan and poly(gamma-glutamic acid) into polyelectrolyte complexes. *Biomacromolecules.* 2011;12(12):4183–95.
 - 59 U.S. Department of Health and Human Services/Food and Drug Administration/Center for Drug Evaluation and Research/Center for Biologics Evaluation and Research/Center for Veterinary Medicine/Center for Devices and Radiological Health/Office of Regulatory Affairs. Guidance for industry: pyrogen and endotoxins testing: questions and answers, 2012.
 - 60 Juenger S, Gantenbein-Ritter B, Lezuo P, Alini M, Ferguson SJ, Ito K. Effect of limited nutrition on in situ intervertebral disc cells under simulated-physiological loading. *Spine.* 2009;34(12):1264–71.
 - 61 Chan SCW, Walser J, Kaeppli P, Shamsollahi MJ, Ferguson SJ, Gantenbein-Ritter B. Region specific response of intervertebral disc cells to complex dynamic loading: an organ culture study using a dynamic torsion-compression bioreactor. *Plos One.* 2013;8(8):e72489.
 - 62 Haschtman D, Stoyanov JV, Ferguson SJ. Influence of diurnal hyperosmotic loading on the metabolism and matrix gene expression of a whole-organ intervertebral disc model. *J Orthop Res.* 2006;24(10):1957–66.
 - 63 Illien-Juenger S, Gantenbein-Ritter B, Grad S, Lezuo P, Ferguson SJ, Alini M, et al. The combined effects of limited nutrition and high-frequency loading on intervertebral discs with endplates. *Spine.* 2010;35(19):1744–52.
 - 64 Paul CPL, Zuiderbaan HA, Doulabi BZ, van der Veen AJ, van de Ven PM, Smit TH, et al. Simulated-physiological loading conditions preserve biological and mechanical properties of caprine lumbar intervertebral discs in ex vivo culture. *Plos One.* 2012;7(3):e33147
 - 65 Wang S-L, Yu Y-L, Tang C-L, Lv F-Z. Effects of TGF-beta 1 and IL-1 beta on expression of ADAMTS enzymes and TIMP-3 in human intervertebral disc degeneration. *Exp Ther Med.* 2013;6(6):1522–6.
 - 66 Zhang R, Ruan D, Zhang C. Effects of TGF-beta1 and IGF-1 on proliferation of human nucleus pulposus cells in medium with different serum concentrations. *J Orthop Surg Res.* 2006;1:9
 - 67 Nishida K, Kang JD, Gilbertson LG, Moon SH, Suh JK, Vogt MT, et al. Modulation of the biologic activity of the rabbit intervertebral disc by gene therapy: an in vivo study of adenovirus-mediated transfer of the human transforming growth factor beta 1 encoding gene. *Spine.* 1999;24(23):2419–25.
 - 68 He E, Cui JH, Li C, Tang C, Kim I-S, Kim Y-W, et al. The combined effects of transforming growth factor-beta and basic fibroblast growth factor on the human degenerated nucleus pulposus cells in monolayer culture. *J Tissue Eng Regen Med.* 2013;10(3):146–54.
 - 69 Lin YH, Chung CK, Chen CT, Liang HF, Chen SC, Sung HW. Preparation of nanoparticles composed of chitosan/poly-gamma-glutamic acid and evaluation of their permeability through Caco-2 cells. *Biomacromolecules.* 2005;6(2):1104–12.
 - 70 Hajdu I, Bodnar M, Filipcsei G, Hartmann JF, Daroczi L, Zrinyi M, et al. Nanoparticles prepared by self-assembly of chitosan and poly-gamma-glutamic acid. *Colloid Polym Sci.* 2008;286(3):343–50.
 - 71 Sogias IA, Khutoryanskiy VV, Williams AC. Exploring the factors affecting the solubility of chitosan in water. *Macromol Chem Phys.* 2010;211(4):426–33.
 - 72 Berger J, Reist M, Mayer JM, Felt O, Gurny R. Structure and interactions in chitosan hydrogels formed by complexation or aggregation for biomedical applications. *Eur J Pharm Biopharm.* 2004;57(1):35–52.
 - 73 Nair LS, Laurencin CT. Biodegradable polymers as biomaterials. *Prog Polym Sci.* 2007;32(8-9):762–98.
 - 74 Rinaudo M. Chitin and chitosan: properties and applications. *Prog Polym Sci.* 2006;31(7):603–32.
 - 75 Suh JKF, Matthew HWT. Application of chitosan-based polysaccharide biomaterials in cartilage tissue engineering: a review. *Biomaterials.* 2000;21(24):2589–98.
 - 76 Di Martino A, Sittinger M, Risbud MV. Chitosan: a versatile biopolymer for orthopaedic tissue-engineering. *Biomaterials.* 2005;26(30):5983–90.
 - 77 Muzzarelli RAA, Greco F, Busilacchi A, Sollazzo V, Gigante A. Chitosan, hyaluronan and chondroitin sulfate in tissue engineering for cartilage regeneration: a review. *Carbohydr Polym.* 2012;89(3):723–39.
 - 78 Alini M, Roughley PJ, Antoniou J, Stoll T, Aebi M. A biological approach to treating disc degeneration: not for today, but maybe for tomorrow. *Eur Spine J.* 2002;11:S215–S20.
 - 79 Cheng Y-H, Yang S-H, Lin F-H. Thermosensitive chitosan-gelatin-glycerol phosphate hydrogel as a controlled release system of ferulic acid for nucleus pulposus regeneration. *Biomaterials.* 2011;32(29):6953–61.
 - 80 Mwale F, Wertheimer MR, Antoniou J. Novel nitrogen rich polymers and chitosan for tissue engineering of intervertebral discs. *Adv Sci Technol.* 2008;57:117–24.
 - 81 Renani HB, Ghorbani M, Beni BH, Karimi Z, Mirhosseini M, Zarkesh H, et al. Determination and comparison of specifics of nucleus pulposus cells of human intervertebral disc in alginate and chitosan-gelatin scaffolds. *Adv Biomed Res.* 2012;1:81
 - 82 Roughley P, Hoemann C, DesRosiers E, Mwale F, Antoniou J, Alini M. The potential of chitosan-based gels containing intervertebral disc cells for nucleus pulposus supplementation. *Biomaterials.* 2006;27(3):388–96.

- 83 Alini M, Eisenstein SM, Ito K, Little C, Kettler AA, Masuda K, et al. Are animal models useful for studying human disc disorders/degeneration? *Eur Spine J*. 2008;17(1):2–19.
- 84 Anderson DG, Albert TJ, Fraser JK, Risbud M, Wuisman P, Meisel HJ, et al. Cellular therapy for disc degeneration. *Spine*. 2005;30(17):S14–S9.
- 85 Huang Y-C, Leung VYL, Lu WW, Luk KDK. The effects of microenvironment in mesenchymal stem cell-based regeneration of intervertebral disc. *Spine J*. 2013;13(3):352–62.
- 86 Oshima H, Ishihara H, Urban JPG, Tsuji H. The use of coccygeal disks to study intervertebral disc metabolism. *J Orthop Res*. 1993;11(3):332–8.
- 87 Bibby SRS, Jones DA, Ripley RM, Urban JPG. Metabolism of the intervertebral disc: Effects of low levels of oxygen, glucose, and pH on rates of energy metabolism of bovine nucleus pulposus cells. *Spine*. 2005;30(5):487–96.
- 88 Peng S-F, Yang M-J, Su C-J, Chen H-L, Lee P-W, Wei M-C, et al. Effects of incorporation of poly(gamma-glutamic acid) in chitosan/DNA complex nanoparticles on cellular uptake and transfection efficiency. *Biomaterials*. 2009;30(9):1797–808.
- 89 Liao ZX, Peng SF, Chiu YL, Hsiao CW, Liu HY, Lim WH, et al. Enhancement of efficiency of chitosan-based complexes for gene transfection with poly(gamma-glutamic acid) by augmenting their cellular uptake and intracellular unpackage. *J Control Release*. 2014;193:304–15.
- 90 Peng SF, Tseng MT, Ho YC, Wei MC, Liao ZX, Sung HW. Mechanisms of cellular uptake and intracellular trafficking with chitosan/DNA/poly(gamma-glutamic acid) complexes as a gene delivery vector. *Biomaterials*. 2011;32(1):239–48.
- 91 Phanse Y, Ramer-Tait AE, Friend SL, Carrillo-Conde B, Lueth P, Oster CJ, et al. Analyzing cellular internalization of nanoparticles and bacteria by multi-spectral imaging flow cytometry. *J Vis Exp*. 2012;(64):3884.
- 92 Horner HA, Urban JPG. 2001 Volvo award winner in basic science studies: Effect of nutrient supply on the viability of cells from the nucleus pulposus of the intervertebral disc. *Spine*. 2001;26(23):2543–9.
- 93 Razaq S, Urban JPG, Wilkins RJ. Regulation of intracellular pH by bovine intervertebral disc cells. *Cell Physiol Biochem*. 2000;10(1-2):109–15.
- 94 Mavrogenatou E, Kletsas D. Differential response of nucleus pulposus intervertebral disc cells to high salt, sorbitol, and urea. *J Cell Physiol*. 2012;227(3):1179–87.
- 95 Mavrogenatou E, Kletsas D. High osmolality activates the G1 and G2 cell cycle checkpoints and affects the DNA integrity of nucleus pulposus intervertebral disc cells triggering an enhanced DNA repair response. *DNA Repair*. 2009;8(8):930–43.
- 96 Gruber HE, Ingram JA, Norton HJ, Hanley EN Jr. Senescence in cells of the aging and degenerating intervertebral disc—Immunolocalization of senescence-associated beta-galactosidase in human and sand rat discs. *Spine*. 2007;32(3):321–7.
- 97 Kim K-W, Chung H-N, Ha K-Y, Lee J-S, Kim Y-Y. Senescence mechanisms of nucleus pulposus chondrocytes in human intervertebral discs. *Spine J*. 2009;9(8):658–66.
- 98 Le Maitre CL, Freemont AJ, Hoyland JA. Accelerated cellular senescence in degenerate intervertebral discs: a possible role in the pathogenesis of intervertebral disc degeneration. *Arthritis Res Ther*. 2007;9(3):R45.
- 99 Roberts S, Evans EH, Kletsas D, Jaffray DC, Eisenstein SM. Senescence in human intervertebral discs. *Eur Spine J*. 2006;15: S312–S6.
- 100 Gantenbein B, Grunhagen T, Lee CR, van Donkelaar CC, Alini M, Ito K. An in vitro organ culturing system for intervertebral disc explants with vertebral endplates—a feasibility study with ovine caudal discs. *Spine*. 2006;31(23):2665–73.
- 101 Illien-Juenger S, Pattappa G, Peroglio M, Benneker LM, Stoddart MJ, Sakai D, et al. Homing of mesenchymal stem cells in induced degenerative intervertebral discs in a whole organ culture system. *Spine*. 2012;37(22):1865–73.
- 102 Furtwaengler T, Chan SCW, Bahrenberg G, Richards PJ, Gantenbein-Ritter B. Assessment of the matrix degenerative effects of MMP-3, ADAMTS-4, and HTRA1, injected into a bovine intervertebral disc organ culture model. *Spine*. 2013;38(22):E1377–E87.
- 103 Spencer GJ, McGrath CJ, Genever PG. Current perspectives on NMDA-type glutamate signalling in bone. *Int J Biochem Cell Biol*. 2007;39(6):1089–104.
- 104 Piepoli T, Mennuni L, Zerbi S, Lanza M, Rovati LC, Caselli G. Glutamate signaling in chondrocytes and the potential involvement of NMDA receptors in cell proliferation and inflammatory gene expression. *Osteoarthr Cartil*. 2009;17(8):1076–83.
- 105 Salter DM, Wright MO, Millward-Sadler SJ. NMDA receptor expression and roles in human articular chondrocyte mechanotransduction. *Biorheology*. 2004;41(3-4):273–81.
- 106 Li HT, Li XH, Liu GZ, Chen JS, Weng XP, Liu FY, et al. *Bauhinia championi* (Benth.) Benth. polysaccharides upregulate Wnt/beta-catenin signaling in chondrocytes. *Int J Mol Med*. 2013;32(6):1329–36.
- 107 Weng XP, Lin PD, Liu FY, Chen JS, Li HT, Huang LC, et al. *Achyranthes bidentata* polysaccharides activate the Wnt/beta-catenin signaling pathway to promote chondrocyte proliferation. *Int J Mol Med*. 2014;34(4):1045–50.